Journal of Environmental Management 294 (2021) 113005

Contents lists available at ScienceDirect

Journal of Environmental Management

journal homepage: www.elsevier.com/locate/jenvman

Comparison of the sorption capacity of basic, acid, direct and reactive dyes by compost in batch conditions

Khaled Al-Zawahreh [a], María Teresa Barral [b], Yahya Al-Degs [c], Remigio Paradelo [b,*]

[a] Department of Earth Sciences and Environment, Prince El-Hassan Bin Talal Faculty of Natural Resources and Environment, The Hashemite University, Zarqa, 13133, Jordan
[b] Department of Soil Science and Agricultural Chemistry, University of Santiago de Compostela, 15782, Santiago de Compostela, Spain
[c] Department of Chemistry, Faculty of Science, The Hashemite University, Zarqa, 13133, Jordan

ARTICLE INFO

Keywords:
Compost
Biosorbents
Textile dyes
Sorption

ABSTRACT

Research on biosorption of organic dyes is an important subject for the development of clean technologies for the treatment of textile wastewater. In this work, the process of sorption of four textile dyes of different natures, namely Basic Violet 10 (BV10), Acid Red 27 (AR27), Direct Blue 151 (DB151) and Reactive Violet 4 (RV4) onto two composts, pine bark compost and municipal solid waste compost, has been studied. For this, sorption kinetics and equilibrium sorption at different solution pH values (3.0–7.0) and salinity (0–1.0 M KCl) conditions have been assessed in batch experiments. Sorption rates were relatively slow for BV10, reaching equilibrium only after 24 h, and faster for the rest: around 5–6 h for RV4 and AR27 and 2 h for DB151. Kinetics of dye sorption followed a pseudo-first order model, except that of DB151, which was better described by a pseudo-second order model. The sequence of adsorption capacity for both composts was as follows: BV10 > DB151 > RV4 > AR27. In general, dye sorption at the equilibrium was adequately described by the Langmuir model, what allows to estimate maximum retention capacities for each dye by the composts. At the best removal conditions, pine bark compost presented maximum sorption capacities of 204 mg g^{-1} for BV10, 54 mg g^{-1} for DB151, 23 mg g^{-1} for RV4, and 4.1 mg g^{-1} for AR27, whereas municipal solid waste compost showed maximum sorption of 74 mg g^{-1} for DB151, 38 mg g^{-1} for RV4, 36 mg g^{-1} for BV10, and 1.6 mg g^{-1} for AR27. Sorption increased at acid pH in all cases, likely because of modification of charges of the dyes and higher electrostatic attraction, whereas increasing salinity also had a positive effect on sorption, attributed to a solute-aggregation mechanism in solution. In conclusion, organic waste-derived products, like composts, can be applied in the removal of colorants from wastewater, although they would be more effective for the removal of basic cationic dyes than other types, due to electrostatic interaction with mostly negatively-charged composts.

1. Introduction

Organic dyes are heavily used in the textile, paper and paint production industries and it has been estimated that 10,000 different textile dyes are available worldwide, with an annual production of around 7×10^5 tons (Crini, 2006). In the textile industry, up to 50% of applied dyes do not bind to the fabrics (Kausar et al., 2018) and are eliminated as colored wastewaters, which should be treated properly before discharging into different water bodies. Colored pollutants have a negative influence on the photosynthetic activity of aquatic life due to their strong visible light absorption (Amin, 2009; Antighin et al., 2015). Moreover, exposure to high levels of some textile dyes can cause severe damage to human beings including kidney, liver, reproductive system, brain and central nervous system (Amin, 2009; Antighin et al., 2015; Kausar et al., 2018). Consequently, treatment of dye-containing effluents is a big challenge for the preservation of environmental quality and the sustainability of textile industries (Kadirvelu et al., 2000).

Among the methods tested for the removal of textile dyes, adsorption from solution has been reported to be efficient in terms of operational costs and ease of design (Nassar and El-Geundi, 1991). Activated carbon is the ideal adsorbent against a wide range of pollutants (Crini, 2006), but its high cost has promoted research for cheaper substitutes, including natural materials of different origins that can be available in large amounts (Nassar and El-Geundi, 1991; Kadirvelu et al., 2000;

* Corresponding author.
E-mail address: remigio.paradelo.nunez@usc.es (R. Paradelo).

https://doi.org/10.1016/j.jenvman.2021.113005
Received 16 March 2021; Received in revised form 6 May 2021; Accepted 2 June 2021
Available online 12 June 2021

Table 1
Chemical properties of the four dyes.

Dye	Molecular formula	Structure	Molecular weight (g mol $^{-1}$)	pKa	Water solubility
Basic Violet 10	$C_{28}H_{31}ClN_2O_3$	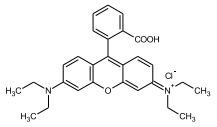	478.5	3.7	8–15 g L^{-1} (20 °C)
Acid Red 27	$C_{20}H_{11}N_2Na_3O_{10}S_3$	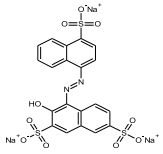	604.5	2.61, 7.41	50 g L^{-1} (20 °C)
Direct Blue 151	$C_{34}H_{25}N_5O_{10}S_2Na_2$	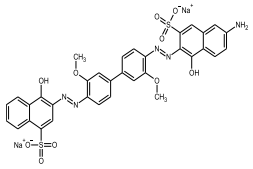	773.7	2.68	High
Reactive Violet 4	$C_{20}H_{16}N_3Na_3O_{15}S_4$	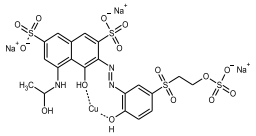	799.1	4.55	High

Table 2
Physicochemical parameters of the composts. CPB: composted pine bark; MSWC: municipal solid waste compost; pH_{ZPC}: pH at point of zero charge; OM: organic matter; AEC: anionic exchange capacity; CEC: cation exchange capacity; SSA: specific surface area.

	CPB	MSWC
pH	5.3	8.5
pH_{ZPC}	4.4	8.2
OM, %	95.3	43.8
C, %	53.6	22.9
N, %	0.93	2.83
C/N ratio	57.6	8.1
CEC, cmol(+) kg^{-1}	25.4	18.8
AEC, cmol(−) kg^{-1}	4.6	3.6
SSA, m^2 g^{-1}	22.4	5.8

Crini, 2006; Hameed and El-Khaiary, 2008; Anastopoulos and Kyzas, 2014, 2015).

Recently, increasing attention has been directed to the use of composts in this field (McKay et al., 2011; Paradelo et al., 2009, 2019, 2020; Pushpa et al., 2016). Compost is an organic material produced after aerobic biological decomposition of organic wastes under specific conditions, in a process called composting. In this process, decomposable organic materials degrade in aerobic atmosphere to be converted into more stable products. Composts are often applied as soil conditioners and fertilizers in gardening, agriculture, landscaping and organic farming and more recently for the removal of pollutants from water through adsorption processes. This application is particularly interesting for composts that are not suitable for agricultural use due to low nutrient contents, high salinity or high levels of metals (Paradelo et al., 2020). Compared to other adsorbents, composts offer interesting advantages such as their lower production cost and high availability, since they are produced from organic-rich-wastes that otherwise would be landfilled, incinerated or dumped in nature (Wang et al., 2020). In addition, because of their low cost they don't need to be regenerated for reuse and they can be disposed, incinerated or even further composted to remove adsorbed dyes (Dey et al., 2017). The few studies that have discussed the removal of textile dyes from solution by composts have reported promising results (McKay et al., 2011; Pushpa et al., 2016; Paradelo et al., 2020), although they have been mostly focused on basic cationic dyes, with very few research done on other types of dyes.

In this work, the performance of two composts of different origin and properties for the removal of acid, basic, direct and reactive textile dyes from solution was investigated. Both kinetic and equilibrium sorption were addressed, as well as the effect of solution pH and salinity on dye removal, in order to determine the potential of these composts as adsorbents in textile wastewater treatment.

2. Materials and methods

2.1. Adsorbates

Four textile dyes were studied, belonging to the main dye classes: basic, acid, direct and reactive. Basic Violet 10 (BV10, also known as rhodamine B) and Acid Red 27 (AR27, also known as amaranth dye) were purchased from Panreac (Barcelona, Spain). Direct Blue 151 (DB151) and Reactive Violet 4 (RV4) were purchased from Sigma–Aldrich® chemicals. The pK_a values of the dyes, determined from the half-pointof pH-V_{NAOH} titration plot of 0.010 M dye solutions, chemical structures and other properties are provided in Table 1. BV10 has no azo bond in its structure and no polar functional groups. AR27 has one azo bond with three ionizable sulfonate groups. DB151 has a large hydrophobic skeleton with two azo bonds, polar groups (N–H, O–H, C–O) and two ionizable sulfonate groups conferring anionic character. RV4 has also an azo dye, with one azo bond, three sulfonate groups, and O–H as polar functional group.

2.2. Biosorbents

Two composts were used in this work, produced in industrial composting facilities in the region of Galicia (Spain). Municipal solid waste compost (MSWC) was obtained by aerobic large-scale composting of source-separated organic fraction of municipal solid waste at the Complexo Medioambiental do Barbanza (A Coruña, Spain). Composted pine bark (CPB) was obtained after aerobic composting of pine bark in windrows and supplied by the company Costiña Orgánica (A Coruña, Spain).

The pH of the composts was measured in a 1:5 (v/v) compost/water suspension. The pH at which the net surface charge on the compost surface is zero (pH of point of zero charge, pH_{pzc}) was measured by the

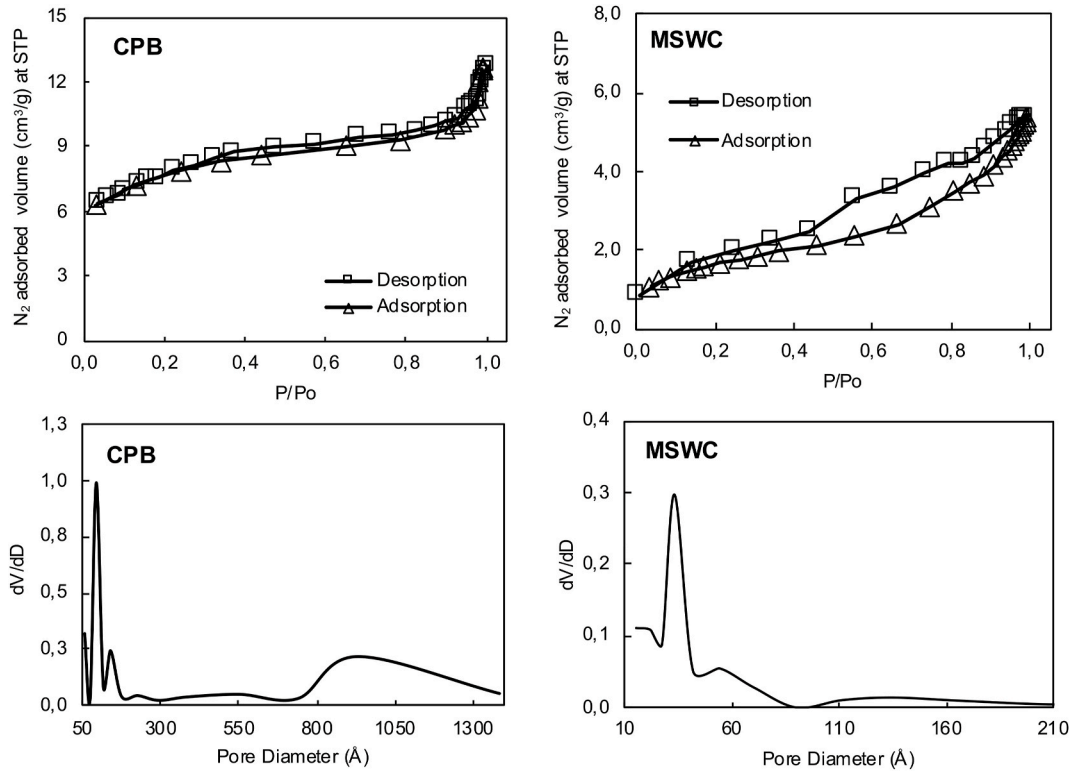

Fig. 1. N_2 adsorption/desorption isotherms and pore size distribution of the composts. CPB: composted pine bark; MSWC: municipal solid waste compost.

pH drift method (Sunjuk et al., 2019). The initial pH (pH_i) of different solutions (25.0 mL of 0.01 M KCl) in conical flasks was adjusted over the range 2.0–10.0 (accuracy ± 0.1 unit) by adding acid or base. To the flasks, 0.25 g compost was added and the final pH (pH_f) was recorded after 24 h shaking at 25 °C. The difference (pH_i - pH_f) was then plotted against pH_i and the pH_{pzc} was estimated as the point at which the difference is zero. Contents of C, H, and N were quantified using CHN elemental analyzer (ELTRA CW multiphase determinator, Italy). Textural characteristics of composts were obtained using standard N_2–adsorption techniques (Quantachrome, Nova, Surface Area and Pore Size Analyzer, USA); specific surface area and pore size distribution were determined following the Barrett-Joyner-Halenda (BJH) method.

2.3. Sorption experiments at different experimental factors

For the sorption experiments, a working stock solution of 1000 mg L^{-1} of each dye was prepared by dissolving an accurately weighed quantity of each single dye in deionized water and subsequently diluting to the needed concentrations.

The effect of contact time on dye removal by compost was studied by shaking 0.5 g of biosorbent with 50 mL of solutions with different dye initial concentrations. Based on previous trials, higher concentrations were used for BV10-CPB and BV10-MSWC tests (500 and 200 and mg L^{-1} respectively) due to the high affinity of this dye for both composts, than for DB151 and RV4 (100 mg L^{-1}) and AR27 sorption (20 mg L^{-1}). The suspensions were shaken during different times (5–1440 min) at 25 °C, and the supernatant was extracted and filtered. The dye concentrations in the extracts were quantified by measuring absorbance in an UV/VIS spectrophotometer (Thermo evolution 100 electro corporation, USA) at 547 nm for Basic Violet 10, 522 nm for Acid Red 27, 554 nm for DB151 and 558 nm for RV4. All tests were carried out in triplicates.

For the study of the equilibrium sorption, batch tests were carried out by shaking 0.50 g of each compost with 50 mL of each individual dye solution at various initial concentrations (10–2000 mg L^{-1} for BV10 and CPB, 2–200 mg L^{-1} for BV10 and MSWC, 2–50 mg L^{-1} for AR27, 5–700 mg L^{-1} for DB151 and 10–500 mg L^{-1} for RV4) in a thermostated shaker (GFL, Germany) at 25 °C and 130 rpm for 24 h. After this period, compost particles were removed by centrifugation at 5000 rpm for 5 min and the clean supernatant was filtered for spectral analysis. The dye concentrations in the extracts (Ce, mg L^{-1}) were determined by spectrophotometry as explained above. All tests were carried out in triplicates. The amount of dye adsorbed by the compost (q_e, mg g^{-1}) was calculated according to Eq. (1):

$$q_e = \frac{(C_o - C_e)V}{m} \quad (1)$$

where V and m are the volume of solution (L) and mass of compost (g), respectively.

The effect of the solution pH on dyes uptake was studied over the range 3.0–7.0 (±0.3) by adjusting the pH of the initial dye solution with 0.5 N NaOH or 0.5 N HCl; the pH was regularly readjusted during the course of sorption tests. The effect of solution salinity on dyes removal was studied at 0.1 and 1.0 M KCl background solution. All tests were carried out in triplicates. The spectra of dyes were insensitive to variations in pH and salinity, so their quantification in the extracts was carried out as explained above.

2.4. IR spectra of composts before and after adsorption

Dye-loaded composts were separated from solution, washed with distilled water, and dried at 105 °C. Then, 100 mg of each compost were thoroughly mixed with 300 mg dried KBr and pressed at 10 bar to produce the disc for the preparation of the spectra. FTIR spectra were obtained within the range 400–4000 cm^{-1} using a PerkinElmer Dynascan Interferometer AVI (Waltham, MA, USA).

2.5. Desorption

For the study of desorption, 500 mg of each compost were suspended

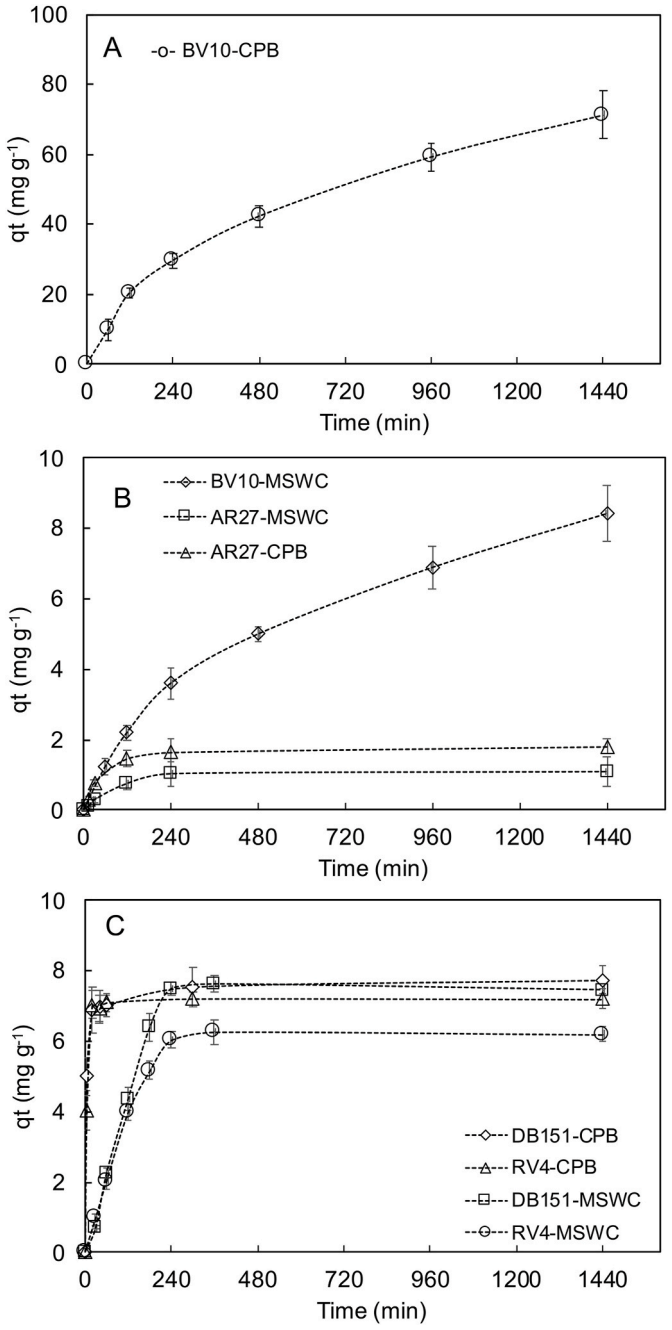

Fig. 2. Kinetics of dye sorption by the composts and fittings to pseudo-first order kinetics. CPB: composted pine bark; MSWC: municipal solid waste compost; BV10: Basic Violet 10; AR27: Acid Red 27; DB151: Direct Blue 151; RV4: Reactive Violet 4.

in 50 mL of dye solutions in triplicate, with initial concentrations of 2000 mg L^{-1} for BV10, 700 mg L^{-1} for DB151, 200 mg L^{-1} for RV4 and 50 mg L^{-1} for AR27. Suspensions were shaken on a rotary shaker at 60 rpm at room temperature (25 ± 1 °C) for 24 h and centrifuged at 4000 *g* for 5 min. The supernatant was removed and the centrifuged residues were weighed to calculate the amount of dye solution occluded in the solid. Then the composts were resuspended in 50 mL of water, shaken again for 24 h and centrifuged. Supernatants were analyzed immediately for dye concentrations as explained above and desorption was expressed as percentage of the previously absorbed dye.

2.6. Fitting of kinetic models

Adsorption kinetics data were described using the Lagergren's pseudo-first order and pseudo-second order models, defined by Equations (2) and (3), respectively:

$$q_a = q_e\left(1 - e^{-k_1 t}\right) \tag{2}$$

$$q_a = \frac{k_2 q_e^2 t}{1 + k_2 q_e t} \tag{3}$$

where q_a (mg g^{-1}) is the amount of dye removed by the compost at a time t, q_e (mg g^{-1}) is the amount of dye removed at equilibrium (this parameter is fitted by the model), k_1 (h^{-1}) is the pseudo-first-order rate constant, and k_2 (g mg^{-1} h^{-1}) is the pseudo-second-order rate constant.

2.7. Adsorption isotherms

Different sorption models were adjusted to isotherms data in order to predict the maximum uptake capacity, formation of multilayer sorption, variability of active sites, porosity, and heterogeneity of sorbent. Among them, only three models were found applicable: Langmuir, Freundlich and Sips models. The Langmuir equation has the following form:

$$q_e = \frac{Q_L K_L C_e}{1 + K_L C_e} \tag{4}$$

where Q_L (mg g^{-1}) and K_L (L mg^{-1}) are respectively the maximum sorption capacity and the affinity constant of the dye toward the compost. The model assumes equal-energy active sites, no interaction with adsorbed solutes, and one mono-layer coverage.

The Freundlich isotherm model expression defines the heterogeneity of the surface as well as the exponential distribution of the active sites and the active sites energies:

$$q_e = K_F C_e^{1/n_F} \tag{5}$$

where K_F (L^n mg^{1-n} g^{-1}) is the Freundlich constant and can indicate uptake capacity, while 1/n (dimensionless) measures favorability of the process and both are system specific constants.

A combination of both Langmuir and Freundlich isotherm models resulted in the Sips isotherm model (Sips, 1948). This leads to the production of an expression that has a finite limit at high concentration:

$$q_e = \frac{Q_S K_S C_e^{n_S}}{1 + K_S C_e^{n_S}} \tag{6}$$

where Q_s (mg g^{-1}), *Ks* (L mg^{-1}), and n_s (dimensionless) are Sips maximum adsorption capacity, Sips equilibrium constant and the model exponent, respectively (Sips, 1948; Ayawei et al., 2017).

The relative error of prediction (REP%) was used as a criterion to select the optimum model as equilibrium data was fitted by more than one model. REP% is estimated as follows (Ayawei et al., 2017):

$$REP\% = 100 \times \left(\frac{\sum_{i=1}^{n} \left(q_{i,pred} - q_{i,act}\right)^2}{\sum_{i=1}^{n} \left(C_{i,act}\right)^2} \right)^{1/2} \tag{7}$$

where $q_{i,pred}$, $q_{i,act}$, and n are predicted sorption value, actual sorption value, and number of experimental points, respectively.

3. Results and discussion

3.1. Characteristics of composts

The main physicochemical parameters of the composts are provided in Table 2 (additional properties can be found in Paradelo et al., 2020).

Table 3
Kinetic parameters for pseudo-first and pseudo-second order models for dyes sorption rates by composts. CPB: composted pine bark; MSWC: municipal solid waste compost; $q_e(exp)$: experimental sorption value at equilibrium (mg g^{-1}); $q_e(model)$: equilibrium sorption value predicted from the model (mg g^{-1}); k_1: pseudo first order model constant (min^{-1}); k_2: pseudo second order model constant (g mg^{-1} min^{-1}); REP%: relative error of prediction.

Dye	Compost	q_e(exp)	Pseudo-first order model			Pseudo-second order model		
			k_1	q_e(model)	REP%	k_2	q_e(model)	REP%
Basic Violet 10	CPB	73.4	0.114	78.5	3.5	0.015	71.5	1.6
	MSWC	10.5	0.084	10.1	4.0	0.010	10.4	1.2
Acid Red 27	CPB	1.79	0.027	1.77	4.5	0.019	1.97	7.3
	MSWC	1.25	0.011	1.22	2.3	0.012	1.35	5.1
Direct Blue 151	CPB	7.71	0.227	7.32	6.4	0.051	7.56	2.7
	MSWC	7.31	0.162	7.22	4.8	0.036	7.22	1.9
Reactive Violet 4	CPB	7.62	0.0073	8.12	3.5	0.001	9.34	6.4
	MSWC	6.41	0.0071	6.61	2.7	0.001	7.65	5.6

These composts have been selected for potential use as biosorbents because of their limited application for agronomic use as organic amendments, which would be the first-choice. In this sense, CPB exhibited a strongly acidic nature and low nutrient levels, whereas MSWC has high salinity (9.4 dS m^{-1}) and heavy metal contents (Paradelo et al., 2020).

The values of pH_{zpc} were 4.4 and 8.1 for CPB and MSWC, respectively (Figure S1, Table 2). This parameter allows estimating the nature of the net surface charge of the adsorbent at different solution pH values and are important to understand the mechanism of interaction between dyes and sorbents (Zhu et al., 2015). Figure S1 shows that CPB has lower positive charge and higher negative charge compared to MSWC. At solution pH > pH_{zpc}, the difference pH_i-pH_f is positive and the net surface charge is therefore negative. Conversely, when solution pH < pH_{zpc}, the difference pH_i-pH_f is negative and the net surface charge is positive because compost functional groups are protonated. Even if at pH_{ZPC} the net charge of the compost can be positive, there are still negative charges, as indicated by the CEC values. In any case, it is obvious that there will be more positive charge at lower pH, promoting the interaction with negatively-charged molecules.

Regarding surface properties (Fig. 1), N_2 adsorption-desorption studies show that both composts exhibited type II isotherm according to IUPAC classification (Rouquerol et al., 1994). This is indicative of the mesoporous to macroporous structure of the material. The absence of microporosity (<2 nm) is expected since composts are not exposed to high temperature (>500 °C), as is the case in commercial activated carbon. Based on multipoint BET analysis, specific surface area of adsorbents were 5.8 and 22.4 m^2 g^{-1} for MSWC and CPB, respectively (Table 2). Pore size analysis confirmed that both composts have macroporous structure with average diameter of 33 Å and 90 Å for MSWC and CPB, respectively. Interestingly, the BJH plot of CPB indicated the presence of pores of diameter 135 Å but in much lower volume compared to those of 90 Å.

3.2. Kinetics of dye sorption

Sorption rates of tested dyes by both composts and modelled kinetic data are provided in Fig. 2 and Table 3. Equilibrium was more rapidly achieved for DB151, RV4 and AR27 than for BV10, which shows a high but slow adsorption capacity, on both composts: equilibrium would be reached at around 24 h for BV10, 5–6 h for RV4 and AR27, and around 2 h for DB151. As shown in Table 3, both pseudo-first and second order models showed good quality for the description of the experimental data, although pseudo-first order model showed a better fit (lower REP% values) for AR27 and RV4, whereas pseudo-second order model was slightly more adequate for BV10 and DB151. The better fit of pseudo-second order model would indicate the presence of two or more types of sorption sites on the surface of composts, whereas fitting to a first-order model suggests only one type of sorption sites or at least a very homogeneous sorption (McKay et al., 2011). Regardless of the adsorbed amounts, only minor differences were observed for kinetics of sorption between the composts, with constant rates consistently higher for CPB than for MSWC. According to these, the kinetics of dye sorption follow the sequence DB151 > BV10 > AR27 ≈ RV4. Our results confirm previous observations indicating that, in general, the kinetics of removal of cationic dyes by composts is higher in comparison with that of direct and reactive dyes (Paradelo et al., 2019; Pushpa et al., 2016; Anastopoulos et al., 2018).

3.3. Equilibrium sorption of dyes under different experimental conditions

3.3.1. Influence of solution pH

Adsorption at equilibrium was assessed at different pH values because textile wastewaters show a wide range for this parameter that controls the electrical charge of sorbate and adsorbent (with variable charge) and could affect the extent and mechanisms of sorption; besides, this allowed to compare sorption in similar pH conditions for both composts, which presented different natural pH values. As shown in Fig. 3, typical L2 isotherms according to the Giles and Smith classification were obtained in all cases. This indicates that dye sorption by composts occurs by forming a single layer, with a high affinity between dyes and composts at low concentrations and surface saturation at higher concentrations, as typical of the Langmuir model. In fact, this model was more accurate than the Freundlich model to describe the experimental data, with REP% lower than 10 in all cases (Table 4). Both composts exhibited higher sorption capacity for the basic dye than for the other types at all pH values, with an overall sequence of adsorption BV10 ≫ DB151 > RV4 > AR27. For BV10, the compost CPB clearly outperformed MSWC; for the other dyes, either there was no difference between composts or MSWC showed a slightly higher sorption. Langmuir maximum capacities Q_L ranged from 1.61 mg g^{-1} for AR27 on MSWC to 127.1 mg g^{-1} for BV10 on CPB and in all cases higher values were obtained in acidic solutions. The increase of dye sorption at lower pH was particularly evident for BV10, DB151 and RV4: retention of these dyes by CPB was 2.2–2.4 times higher at pH 3.0 than at pH 7.0. This effect of solution pH on the removal of anionic dyes has been consistently reported in the literature (Chinoune et al., 2016; Tan and Hameed, 2017; Sunjuk et al., 2019).

In order to understand the effect of pH on dye sorption and the mechanisms at different pH values, it must be remembered how solution pH controls simultaneously the net surface charge of the composts and the extent of dye ionization and therefore their charge. To assist in this analysis, the net charge of compost and dyes at the three pH values tested were estimated using the values of the zero point of charge (pH_{zpc}) of the composts and the pKa of the dyes (Table S1, Supplementary material). In the case of DB151 and AR27, the dyes would be negatively charged at all the tested pH values, while the sorbent CPB would be positively charged at pH 3, and negatively charged at pH 5 and 7, giving a plausible explanation to the maximal dye removal at pH 3 (Table 4). For the same reason, the better performance of MSWC than CPB at pH 3.0 could be attributed to the higher net positive charge of this compost.

In turn, in the case of RV4, composts and dye would present net

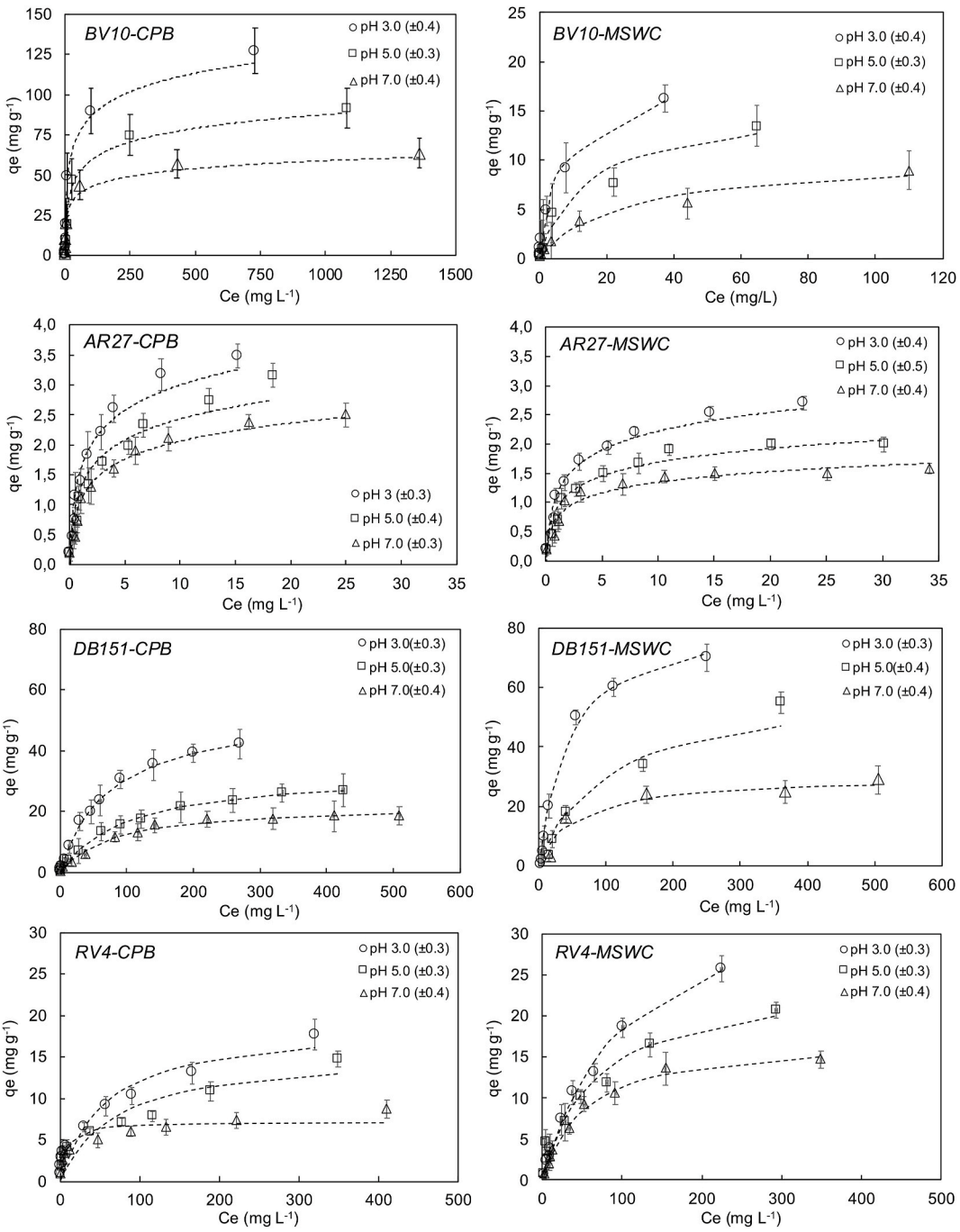

Fig. 3. Sorption isotherms of dyes measured at different pH conditions. The lines represent Langmuir's model. CPB: composted pine bark; MSWC: municipal solid waste compost; BV10: Basic Violet 10; AR27: Acid Red 27; DB151: Direct Blue 151; RV4: Reactive Violet 4.

charges of opposite sign only for MSWC at pH 5.0 and 7.0. However, these were not the conditions producing the highest retention, so it is clear that electrostatic interaction cannot be the main mechanism involved in sorption. Examining the case of BV10, maximum sorption was found at pH 3.0, for which sorbent and sorbate have similar positive net charge, so lower electrostatic interaction (and therefore lower removal capacity) than at higher pH values could be expected, but this was not the case. At pH 5.0 and 7.0, BV10 is present as zwitterion, an electrically neutral chemical compound with positive and negative charges on different atoms (Figure S2, Supplementary material). Although the zwitterion can contribute to retention through a cation exchange mechanism, experimental results indicated a strong reduction in dye uptake at higher pH values. The lower interaction of BV10 with different sorbents at pH > 3.0 has indeed been observed in the literature, what it has been attributed to zwitterion aggregation, due to the attractive electrostatic interactions between the carboxyl and xanthene groups of different molecules, in large dimer clusters that reduce electrostatic interaction and cannot penetrate inside the pores of the sorbents (Yu et al., 2013; Zamouche and Hamdaoui, 2012; Hou et al., 2011).

The fact that dyes sorption changed with pH always in the same direction, despite the diverse situations of electric charge of sorbents and dyes, proves that electrostatic interaction cannot be the only or the main mechanism for the interaction between dyes and compost. Considering the complex structure of the dye molecules, the contribution of other mechanisms such as hydrophobic-hydrophobic and dipole-dipole forces

Table 4
Isotherm parameters for dye sorption under different solution pH. CPB: composted pine bark; MSWC: municipal solid waste compost; Q_L: Langmuir maximum capacity (mg g^{-1}); K_L: Langmuir constant (L g^{-1}); K_F: Freundlich constant (L g^{-1}); n: Freundlich coefficient.

			Langmuir			Freundlich		
Dye	Compost	pH	Q_L	K_L	REP%	K_f	n	REP%
Basic Violet 10	CPB	3.0	127.1	0.039	1.5	13.4	2.78	2.3
		5.0	89.3	0.037	3.4	12.3	3.23	6.7
		7.0	53.5	0.032	2.6	11.9	4.35	8.5
	MSWC	3.0	19.3	0.130	1.2	3.11	2.17	1.4
		5.0	15.4	0.107	1.4	1.92	2.08	2.5
		7.0	10.3	0.089	1.6	1.03	2.08	1.7
Acid Red 27	CPB	3.0	3.89	0.513	3.4	1.33	2.63	5.4
		5.0	3.38	0.489	5.3	1.01	2.56	3.7
		7.0	2.63	0.437	1.8	0.95	3.13	6.7
	MSWC	3.0	2.85	0.488	2.5	1.01	2.94	4.3
		5.0	2.14	0.511	3.1	0.83	3.45	3.2
		7.0	1.61	0.561	3.8	0.73	4.17	5.0
Direct Blue 151	CPB	3.0	53.9	0.0134	2.95	–	–	–
		5.0	33.2	0.0100	5.41	–	–	–
		7.0	22.5	0.0120	5.77	–	–	–
	MSWC	3.0	74.3	0.0195	7.79	–	–	–
		5.0	61.8	0.0162	8.33	–	–	–
		7.0	30.1	0.0189	7.76	–	–	–
Reactive Violet 4	CPB	3.0	19.2	0.0173	7.32	–	–	–
		5.0	15.5	0.0155	8.12	–	–	–
		7.0	7.2	0.0126	7.56	–	–	–
	MSWC	3.0	37.7	0.011	5.33	–	–	–
		5.0	24.7	0.012	7.19	–	–	–
		7.0	17.4	0.014	3.45	–	–	–

should be envisaged to explain dye sorption under unfavorable charge conditions. Hydrophobic interaction between the organic dyes and organic matter-rich composts is possible and could explain the higher affinity of dyes toward CPB over all pH values, taking into account the much higher organic matter content of CPB with respect to MSWC.

3.3.2. *Influence of solution salinity*

Regarding the influence of solution salinity on dye uptake, sorption isotherms at different KCl concentrations are displayed in Fig. 4, whereas estimated parameters for the sorption models are given in Table 5. All the sorption isotherms presented L-type curves that were in general best described by the Langmuir model, with the exceptions of the curves for BV10 and DB151 at the highest salinity (1.0 M KCl), for which the high retention produced H-type isotherms that were better described by the Freundlich or Sips models. In all cases, increasing salinity had a favorable effect on dye sorption that was in general more pronounced for DB151 than for the other dyes, with the weakest effect on AR27. This positive influence of salinity on the removal of anionic dyes from water has already been reported in the literature and attributed to the dimerization of dyes at high ionic strength, which reduces dye solubility and increases sorption as a result (Zamouche and Hamdaoui, 2012; Al-Ghouti et al., 2016; Sunjuk et al., 2019). This dimerization can be due to an increase in intermolecular forces, such as dipole–dipole, ion–dipole or van der Waals dispersion forces at high salinity, which produce a reduction of the repulsive interaction between dyes (Al-Degs et al., 2008; Fedoseeva et al., 2010).

For the interpretation of these results, it has to be taken into account that the modification of salinity affects the pH of the suspensions, so the simultaneous effect of both parameters must be considered together. Increasing salinity affected pH in opposite directions depending on the compost considered: pH became more acid for CPB and more alkaline for MSWC. This is an effect of the displacement by K^+ of the ions present in the exchange complex of the sorbents. In the case of CPB, which has a very acid pH, these cations are mostly protons that reduce solution pH when displaced, whereas for MSWC, with an alkaline pH, K^+ replaces base cations like Ca^{2+} and Mg^{2+} that increase pH when released to the solution. Table S2 (Supplementary material) summarizes the sign of the net charge of composts along with ionization states of dyes under the different conditions of solution pH and KCl concentrations. Comparison with the results of the sorption tests evidences again that electrostatic interaction is not the only or main mechanism involved in retention of anionic dyes. For example, the highest sorption of BV10 by CPB was observed at 1.0 M KCl, where both CPB and BV10 carry net positive charge. In the case of AR27 and DB151, net charges of opposite sign exist only for CPB and not for MSWC, so electrostatic interaction cannot explain why sorption always increased with salinity for both composts. This is definitely not the case either for RV4, where dominant electrostatic interaction is not possible under any conditions due to charges of similar sign in sorbate and sorbent. In summary, as already stated when discussing the effect of pH, hydrophobic interactions or dipole-dipole forces are likely mechanisms that can contribute to dye sorption under unfavorable charge conditions.

In this sense, the FTIR spectra of the dye-loaded composts can help elucidating the interaction mechanisms by evidencing structural changes in the composts after dye sorption. The main modifications observed in the spectra (Fig. 5) include reductions in the bands at 1600 cm^{-1} (corresponding to C═C bonds in lignin) and at 3000-3500 cm^{-1} (O–H bonds in alcohol and carboxylic acid groups), showing interaction of dyes with different functional groups of the organic matter. The detection of the band characteristic of azo bond in the region of 1400–1500 cm^{-1} indicates the presence of –N═N– on the surface of the sorbents (Hu et al., 2003), excluding dye degradation under the tested conditions. The high reduction in the band interval 2000-2300 cm^{-1} for CPB is attributed to hydrophobic-hydrophobic interaction between dyes and this compost. Finally, reductions in the intensity of the 1000-1100 cm^{-1} band for MSWC but not for CPB are likely due to interaction of dyes with the inorganic components of MSWC (that are absent in CPB) since this band corresponds to Al–O bonds in clay minerals and Fe–O in oxides.

3.4. *Desorption*

Finally, desorption of dyes from the composts was studied. As shown in Fig. 6, percentages of desorption for the dyes DB151 and RV4 were very similar without differences between the two composts (values around 11–13% in all cases). Regarding AR27 and BV10, differences were found between the two composts, with lower dye desorption from CPB in the two cases, indicating stronger interaction of both dyes with

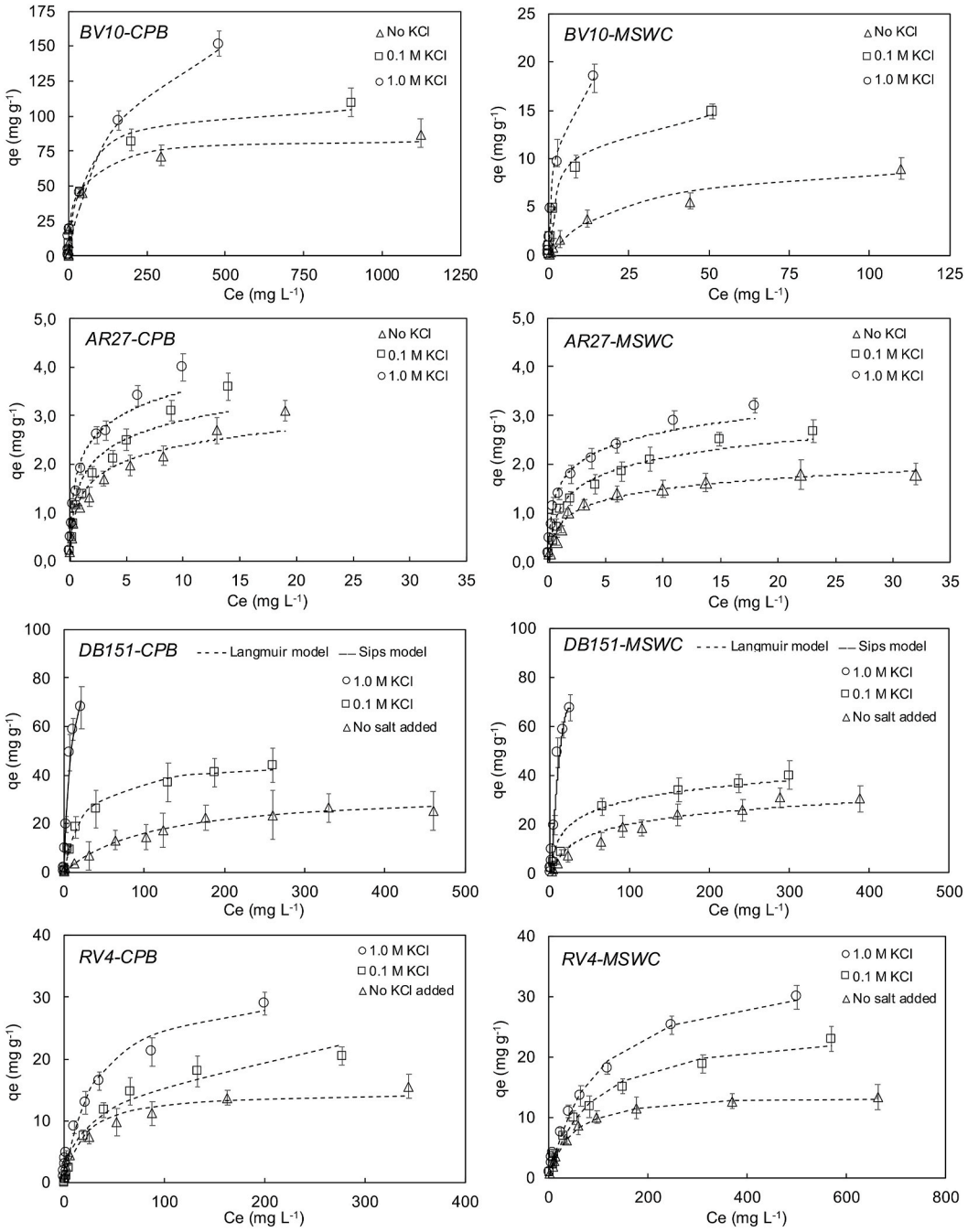

Fig. 4. Sorption isotherms of tested dyes at different salinities. CPB: composted pine bark; MSWC: municipal solid waste compost; BV10: Basic Violet 10; AR27: Acid Red 27; DB151: Direct Blue 151; RV4: Reactive Violet 4.

this compost. Overall, desorption results reflects what has been observed in the equilibrium sorption studies in what concerns the relative affinity of the composts for each dye.

3.5. Comparison of compost performance with other sorbents

When the overall performance of the two composts in this study is compared with other sorbents, in order to assess their suitability for dye removal applications, different situations exist depending on the dye considered. For the basic dye BV10, composted pine bark presented maximum sorption capacity of 127 mg g^{-1} at pH 3, which increased to 205 mg g^{-1} with 1M KCl solution, also at a pH close to 3; however, MSWC presented a poorer performance, with a maximum sorption at 1.0 M KCl of 36.1 mg g^{-1}. The sorption capacity of CPB is promising as these values are not very different from the values of 155 and 264 mg g^{-1} obtained for more expensive synthetic adsorbents like graphene oxides and activated carbon (Yu et al., 2013) and higher than the values of 13.2 and 46.1 mg g^{-1} reported for the natural adsorbents zeolite and kaolinite (Yu et al., 2013), or the 27.2 mg g^{-1} obtained by Jóźwiak et al. (2013) for a sewage sludge and plant residue compost.

In contrast, both composts showed low affinity for the acid dye AR27, with maximum sorption capacities of 4.1 mg g^{-1} and 3.3 mg g^{-1} for CPB and MSWC, respectively. This represents a low removal capacity of both composts when compared to the performance of other adsorbents in the literature, either synthetic sorbents such as graphene nanocomposites with a saturation value of 294 mg g^{-1} (Behnajady, 2014) or residual biosorbents such as water hyacinth leaves, with a maximum sorption of 69 mg g^{-1} (Guerrero-Coronilla et al., 2015).

Table 5
Isotherm parameters for dye sorption under different solution salinity. CPB: composted pine bark; MSWC: municipal solid waste compost; Q_L: Langmuir maximum capacity (mg g^{-1}); K_L: Langmuir constant (L g^{-1}); K_F: Freundlich constant (L g^{-1}); n: Freundlich coefficient; Q_s: Sips saturation value (mg g^{-1}); K_s: Sips model constant; n_s: Sips model exponent.

			Langmuir			Freundlich			Sips			
Dye	Compost	M KCl	Q_L	K_L	REP%	K_f	n	REP%	Q_s	K_s	n_s	REP%
Basic Violet 10	CPB	0	84.1	0.032	1.6	12.0	3.85	1.3	–	–	–	–
		0.1	110.2	0.029	1.5	13.7	3.23	1.2	–	–	–	–
		1.0	204.7	0.031	1.7	15.2	2.78	5.3	–	–	–	–
	MSWC	0	11.2	0.088	1.5	1.62	2.13	3.4	–	–	–	–
		0.1	16.0	0.093	4.4	3.10	2.44	3.4	–	–	–	–
		1.0	36.1	0.091	5.6	5.59	2.22	5.6	–	–	–	–
Acid Red 27	CPB	0	3.12	0.421	6.3	1.04	2.78	3.1	–	–	–	–
		0.1	3.73	0.522	4.9	1.30	2.56	1.9	–	–	–	–
		1.0	4.11	0.613	5.3	1.67	2.56	3.2	–	–	–	–
	MSWC	0	1.93	0.518	5.4	0.78	3.57	4.1	–	–	–	–
		0.1	2.78	0.571	3.7	0.92	2.86	3.7	–	–	–	–
		1.0	3.34	0.592	4.8	1.31	3.03	4.4	–	–	–	–
Direct Blue 151	CPB	0	33.6	0.0092	6.78	–	–	–	–	–	–	–
		0.1	46.3	0.0392	5.68	–	–	–	–	–	–	–
		1.0	–	–	–	–	–	–	70.3	0.0034	2.67	8.89
	MSWC	0	43.8	0.0065	6.86	–	–	–	–	–	–	–
		0.1	47.4	0.0156	8.51	–	–	–	–	–	–	–
		1.0	–	–	–	–	–	–	71.2	0.0586	1.83	7.22
Reactive Violet 4	CPB	0	14.9	0.0318	4.37	–	–	–	–	–	–	–
		0.1	23.3	0.0294	5.37	–	–	–	–	–	–	–
		1.0	32.0	0.0332	6.49	–	–	–	–	–	–	–
	MSWC	0	14.3	0.0223	3.11	–	–	–	–	–	–	–
		0.1	25.0	0.0119	7.01	–	–	–	–	–	–	–
		1.0	35.1	0.0104	5.78	–	–	–	–	–	–	–

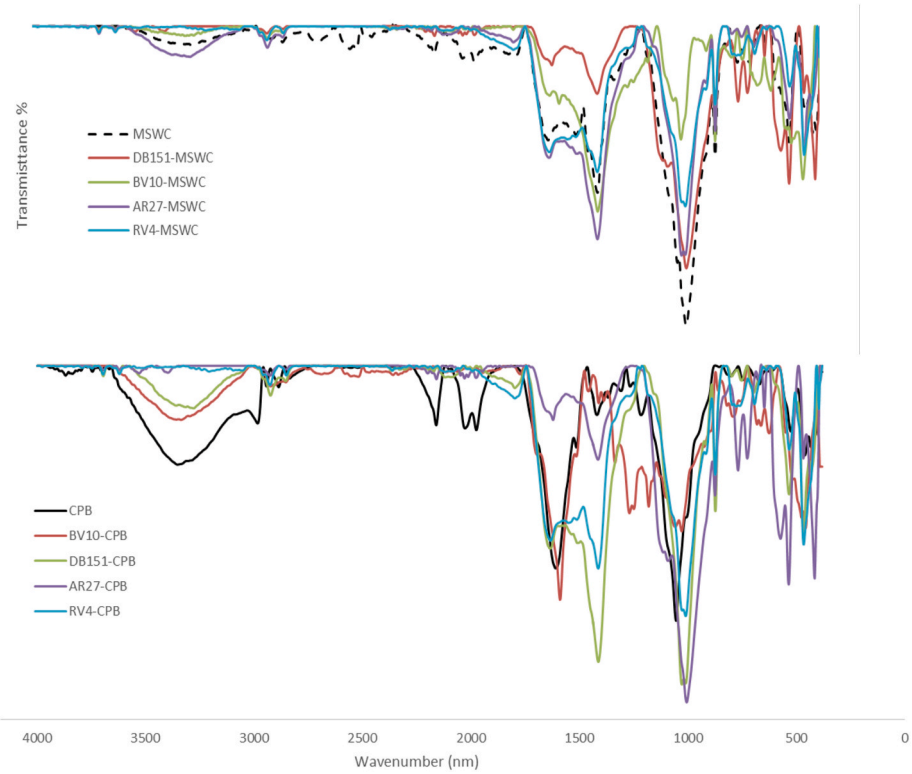

Fig. 5. FTIR spectra of composts before and after dye sorption. CPB: composted pine bark; MSWC: municipal solid waste compost; BV10: Basic Violet 10; AR27: Acid Red 27; DB151: Direct Blue 151; RV4: Reactive Violet 4. (For interpretation of the references to color in this figure legend, the reader is referred to the Web version of this article.)

Assessing the performance of the composts for DB151 and RV4 is more difficult due to the scarcity of sorption studies with these specific molecules. In the case of RV4, the maximum sorption capacities found in our work (32 mg g^{-1} for CPB and 37.7 mg g^{-1} for MSWC) are much lower than those obtained for a starch/polyaniline nanocomposite (578 mg g^{-1}) in the only study published with this dye (Janaki et al., 2012). In the case of DB151, there are no works in the literature that studied the sorption of this dye, but indirect comparison could be made, with caution, using studies dealing with the very similar molecule Direct Blue 71. For this dye, maximum sorption capacities reported include 47–59

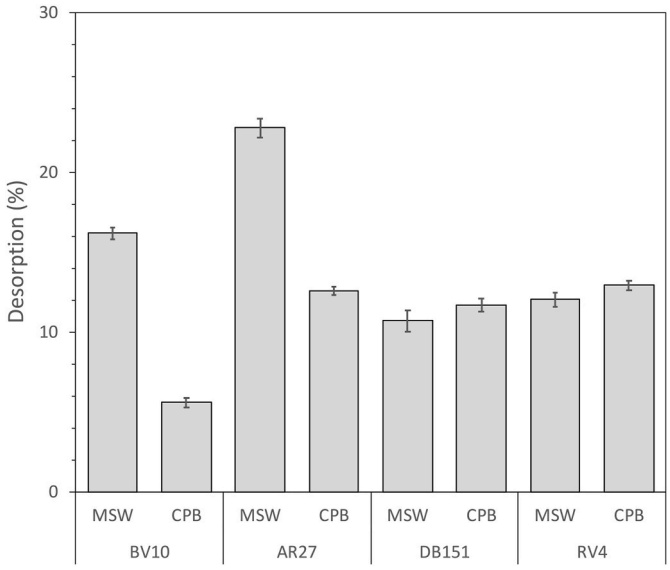

Fig. 6. Desorption percentages of previously adsorbed dye after contact with compost (mean ± standard deviation, n = 3). MSWC: municipal solid waste compost; CPB: composted pine bark.

mg g^{-1} on synthetic alumina/silica oxides (Wawrzkiewicz et al., 2015a, 2015b, 2015b), 45 mg g^{-1} on wheat shells (Buliut et al., 2007) or 61 mg g^{-1} on chitosan/SiO_2/carbon nanotubes (Abasi, 2017), which are similar to the maximum sorption capacities obtained in our study for DB151 (74 mg g^{-1} for MSWC and 54 mg g^{-1} for CPB).

The performance of the composts in this work against different dyes is in agreement with conclusions obtained in a previous review of the use of compost for dye removal, which showed a higher affinity of compost biosorbents for basic dyes than for other types of dyes (Paradelo et al., 2019). Overall, these results suggest that, in comparison with other materials, composts would be a good choice for the treatment of cationic dyes (basic dyes) in wastewater, but not for acid dyes, while their potential use for direct and reactive dyes still needs further research, as the number of published studies to this date is insufficient.

4. Conclusions

A pine bark compost and a municipal solid waste compost have been tested as potential adsorbents for the removal of four different types of textile dyes from aqueous solutions: a basic dye (BV10), an acid dye (AR27), a direct dye (DB151) and a reactive dye (RV4). Sorption was faster for the direct dye than for the other types, followed by the acid and reactive dye, with cationic dye as the slowest. Kinetics of sorption were adequately described by a pseudo-first order model in all cases, although for DB151 it was better fitted by the pseudo-second order model, whereas equilibrium sorption followed in general the Langmuir model. Solution pH and KCl concentration influenced sorption of the four dyes in the same direction for both composts: decrease of pH and increase of salinity improved removal capacity in all cases, so both biosorbents would be more efficient for dye removal from acid wastewaters with high salinity. The results indicate that electrostatic attraction may be important for sorption, but other mechanisms, in particular hydrophobic interactions, must be involved in the process of dye removal. The maximum sorption capacities of the composts followed the sequence BV10 > DB151 > RV4 > AR27, and comparisons to the performance of other biosorbents allow to conclude that composts are a promising material for application in the adsorptive removal of basic dyes, but not for acid dyes, while their potential use with other types of dyes needs further study.

Declaration of competing interest

The authors declare that they have no known competing financial interests or personal relationships that could have appeared to influence the work reported in this paper.

Acknowledgements

Technical assistance by Mr. Bassem Nasrallah (Chemistry Department, Hashemite University, Jordan) is highly appreciated. Dr. Paradelo thanks the Spanish Ministry of Economy and Competitiveness (MINECO) for his Ramón y Cajal fellowship (RYC-2016-19286).

Appendix A. Supplementary data

Supplementary data to this article can be found online at https://doi.org/10.1016/j.jenvman.2021.113005.

Author contributions

Khaled Al-Zawahreh: Methodology, Validation, Formal analysis, Investigation, Resources, Data curation, Writing – original draft, Writing – review & editing, Visualization, Project administration, María Teresa Barral: Conceptualization, Methodology, Resources, Writing – review & editing, Supervision, Project administration, Yahya Al-Degs: Methodology, Writing – review & editing, Remigio Paradelo: Conceptualization, Methodology, Validation, Investigation, Resources, Writing – review & editing, Visualization, Supervision, Project administration, Funding acquisition.

References

Abasi, M., 2017. Synthesis and characterization of magnetic nanocomposite of chitosan/SiO_2/carbon nanotubes and its application for dyes removal. J. Clean. Prod. 145, 105–113. https://doi.org/10.1016/j.jclepro.2017.01.046.

Al-Degs, Y., El-Barghouthi, M., El-Sheikh, A., Walker, G., 2008. Effect of solution pH, ionic strength, and temperature on adsorption behavior of reactive dyes on activated carbon. Dyes Pigments 77, 16–23. https://doi.org/10.1016/j.dyepig.2007.03.001.

Al-Ghouti, M., Issa, A., Al-Saqarat, B., Al-Reyahi, A., Al-Degs, Y., 2016. Multivariate analysis of competitive adsorption of food dyes by activated pine wood. Desal. Wat. Treat. 57, 27651–27662. https://doi.org/10.1080/19443994.2016.1174742.

Amin, N.K., 2009. Removal of direct blue-106 dye from aqueous solution using new activated carbons developed from pomegranate peel: adsorption equilibrium and kinetics. J. Hazard Mater. 165, 52–62. https://doi.org/10.1016/j.jhazmat.2008.09.067.

Anastopoulos, I., Kyzas, G.Z., 2014. Agricultural peels for dye adsorption: a review of recent literature. J. Mol. Liq. 200, 381–389. https://doi.org/10.1016/j.molliq.2014.11.006.

Anastopoulos, I., Kyzas, G.Z., 2015. Composts as biosorbents for decontamination of various pollutants: a review. Water Air Soil Pollut. 226, 61–72. https://doi.org/10.1007/s11270-015-2345-2.

Anastopoulos, I., Margiotoudis, I., Massas, I., 2018. The use of olive tree pruning waste compost to sequestrate methylene blue dye from aqueous solution. Int. J. Phytoremediation 20, 831–838. https://doi.org/10.1080/15226514.2018.1438353.

Antighin, S., Chirila, L., Popescu, A., 2015. Environmentally friendly techniques for wool dyeing process. Acta Chem. Iasi 23, 65–76.

Ayawei, N., Ebelegi, A., Wankasi, D., 2017. Modelling and interpretation of adsorption isotherms. J. Chem., e3039817 https://doi.org/10.1155/2017/3039817.

Behnajady, M., 2014. Investigation on adsorption capacity of TiO_2-P25 nanoparticles in the removal of a mono-azo dye from aqueous solution: a comprehensive isotherm analysis. Chem. Ind. Chem. Eng. Q. 20, 97–107. https://doi.org/10.2298/CICEQ120610105B.

Buliut, Y., Gözübenli, N., Aydin, H., 2007. Equilibrium and kinetics studies for adsorption of direct blue 71 from aqueous solution by wheat shells. J. Hazard Mater. 144 (1–2), 300–306. https://doi.org/10.1016/j.jhazmat.2006.10.027.

Chinoune, K., Bentaleb, K., Bouberka, Z., Nadim, A., Maschke, U., 2016. Adsorption of reactive dyes from aqueous solution by dirty bentonite. Appl. Clay Sci. 123, 64–75. https://doi.org/10.1016/j.clay.2016.01.006.

Crini, G., 2006. Non-conventional low-cost adsorbents for dye removal: a review. Bioresour. Technol. 97, 1061–1085. https://doi.org/10.1016/j.biortech.2005.05.001.

Dey, M.D., Das, S., Kumar, R., Doley, R., Bhattacharya, S.S., Mukhopadhyay, R., 2017. Vermiremoval of methylene blue using *Eisenia fetida*: a potential strategy for bioremediation of synthetic dye-containing effluents. Ecol. Eng. 106, 200–208. https://doi.org/10.1016/j.ecoleng.2017.05.034.

Fedoseeva, M., Fita, P., Punzi, A., Vauthey, E., 2010. Salt effect on the formation of dye aggregates at liquid/liquid interfaces studied by time-resolved surface second harmonic generation. J. Phys. Chem. C 114, 13774–13781. https://doi.org/10.1021/jp104334g.

Guerrero-Coronilla, I., Morales-Barrera, L., Cristiani-Urbina, E., 2015. Kinetic, isotherm and thermodynamic studies of amaranth dye biosorption from aqueous solution onto water hyacinth leaves. J. Environ. Manag. 152, 99–108. https://doi.org/10.1016/j.jenvman.2015.01.026.

Hameed, B., El-Khaiary, M., 2008. Equilibrium, kinetics and mechanism of malachite green adsorption on activated carbon prepared from bamboo by K_2CO_3 activation and subsequent gasification with CO_2. J. Hazard Mater. 157, 344–351. https://doi.org/10.1016/j.jhazmat.2007.12.105.

Hou, M., Ma, C., Zhang, W., Tang, X., Fan, Y., Wan, H., 2011. Removal of rhodamine B using iron-pillared bentonite. J. Hazard Mater. 186, 1118–1123. https://doi.org/10.1016/j.jhazmat.2010.11.110.

Hu, C., Yu, J., Hao, Z., Wong, P., 2003. Photocatalytic degradation of triazine-containing azo dyes in aqueous TiO_2 suspensions. Appl. Catal., B 42, 47–55. https://doi.org/10.1016/S0926-3373(02)00214-X.

Janaki, V., Vijayaraghavan, K., Oh, B.-T., Lee, K.-J., Muthuchelian, K., Ramasamy, A.K., Kamala-Kannan, S., 2012. Starch/polyaniline nanocomposite for enhanced removal of reactive dyes from synthetic effluent. Carbohydr. Polym. 90, 1437–1444 s://doi.org/10.1016/j.carbpol.2012.07.012.

Jóźwiak, T., Filipkowska, U., Rodziewicz, J., Mielcarek, A., Owczarkowska, D., 2013. Application of compost as a cheap sorbent for dyes removal from aqueous solutions. Rocz. Ochr. Sr. 15, 2398–2411.

Kadirvelu, K., Palonival, M., Kalpana, R., Rajeswari, S., 2000. Activated carbon from an agricultural by-product, for the treatment of dyeing industry wastewater. Bioresour. Technol. 74, 263–265. https://doi.org/10.1016/S0960-8524(00)00013-4.

Kausar, A., Iqbal, M., Javed, A., Aftab, K., Nazli, Z., Bhatti, H., Nouren, S., 2018. Dyes adsorption using clay and modified clay: a review. J. Mol. Liq. 256, 395–407. https://doi.org/10.1016/j.molliq.2018.02.034.

McKay, G., Hadi, M., Samadi, M.T., Rahmani, A.R., Aminabad, M.S., Nazemi, F., 2011. Adsorption of reactive dye from aqueous solutions by compost. Desal. Wat. Treat. 28, 164–173. https://doi.org/10.5004/dwt.2011.2216.

Nassar, M., El-Geundi, M., 1991. Comparative cost of colour removal from textile effluents using natural adsorbents. J. Chem. Technol. Biotechnol. 50, 257–264. https://doi.org/10.1002/jctb.280500210.

Paradelo, R., Moldes, A.B., Barral, M.T., 2009. Treatment of red wine vinasses with non-conventional substrates for removing coloured compounds. Water Sci. Technol. 58, 1585–1592. https://doi.org/10.2166/wst.2009.166.

Paradelo, R., Vecino, X., Moldes, A.B., Barral, M.T., 2019. Potential use of composts and vermicomposts as low-cost adsorbents for dye removal: an overlooked application. Environ. Sci. Pollut. Res. 26, 21085–21097. https://doi.org/10.1007/s11356-019-05462-x.

Paradelo, R., Al-Zawahreh, K., Barral, M.T., 2020. Utilization of composts for adsorption of methylene blue from aqueous solutions: kinetics and equilibrium studies. Materials 13, e2179. https://doi.org/10.3390/ma13092179.

Pushpa, T., Vijayaraghavan, J., Jegan, J., 2016. Utilization of Effective Microorganisms based water hyacinth compost as biosorbent for the removal of basic dyes. Desal. Wat. Treat. 57, 24368–24377. https://doi.org/10.1080/19443994.2016.1143405.

Rouquerol, J., Avnir, D., Fairbridge, C., Everett, D., Haynes, J., Pernicone, N., Ramsay, J., Sing, K., Unger, K., 1994. Recommendations for the characterization of porous solids. Pure Appl. Chem. 66, 1739–1758. https://doi.org/10.1351/pac199466081739.

Sips, R., 1948. On the structure of a catalyst surface. J. Chem. Phys. 16, 490–495. https://doi.org/10.1063/1.1746922.

Sunjuk, M., Arar, H., Mahmoud, W., Majdalawi, M., Krishan, M., Abu Salha, Y., El-Eswed, B., 2019. Adsorption of cationic and anionic organic dyes on SiO_2/CuO composite. Desal. Wat. Treat. 169, 383–394. https://doi.org/10.5004/dwt.2019.24706.

Tan, K., Hameed, H., 2017. Insight into the adsorption kinetics models for the removal of contaminants from aqueous solutions. J. Taiwan Inst. Chem. E. 74, 25–48. https://doi.org/10.1016/j.jtice.2017.01.024.

Wang, Z., Bai, F., Chadwick, D., Brook, T., Ma, L., 2020. The progress of composting technologies from static heap to intelligent reactor: benefits and limitations. J. Clean. Prod. 270, 122328. https://doi.org/10.1016/j.jclepro.2020.122328.

Wawrzkiewicz, M., Nowacka, M., Klapiszewski, L., Hubicki, Z., 2015a. Treatment of wastewaters containing acid, reactive and direct dyes using aminosilane functionalized silica. Open Chem 13, 82–95. https://doi.org/10.1515/chem-2015-0013.

Wawrzkiewicz, M., Wiśniewska, M., Gun'koc, V.M., Zarkoc, V.I., 2015b. Adsorptive removal of acid, reactive and direct dyes from aqueous solutions and wastewater using mixed silica–alumina oxide. Powder Technol. 278, 306–315. https://doi.org/10.1016/j.powtec.2015.03.035.

Yu, Y., Murthy, B., Shapter, J., Constantopoulos, K., Voelcker, N., Ellis, A., 2013. Benzene carboxylic acid derivatized graphene oxide nanosheets on natural zeolites as effective adsorbents for cationic dye removal. J. Hazard Mater. 260, 330–338. https://doi.org/10.1016/j.jhazmat.2013.05.041.

Zamouche, M., Hamdaoui, O., 2012. Sorption of Rhodamine B by cedar cone: effect of pH and ionic strength. Energy Procedia 18, 1228–1239. https://doi.org/10.1016/j.egypro.2012.05.138.

Zhu, B., Xia, P., Ho, W., Yu, J., 2015. Isoelectric point and adsorption activity of porous g-C_3N_4. Appl. Surf. Sci. 344, 188–195. https://doi.org/10.1016/j.apsusc.2015.03.086.